preprint; to appear in “Fundamental Physics of Ferroelectrics 2003" (AIP Conference Proceedings Series), (2003).

First Principles Calculations of Ionic Vibrational Frequencies in $PbMg_{1/3}Nb_{2/3}O_3$

S. A. Prosandeev*†, E. Cockayne* and B. P. Burton*

*Ceramics Division, Materials Science and Engineering Laboratory, National Institute of Standards and Technology, Gaithersburg, Maryland 20899-8520
†Physics Department, Rostov State University, 5 Zorge St., 344090 Rostov on Don, Russia

Abstract. Lattice dynamics for several ordered supercells with composition $PbMg_{1/3}Nb_{2/3}O_3$ (PMN) were calculated with first-principles frozen phonon methods. Nominal symmetries of the supercells studied are reduced by lattice instabilities. Lattice modes corresponding to these instabilities, equilibrium ionic positions, and simulated infrared (IR) reflectance spectra are reported.

There is ample evidence of 1:1 (NaCl-type; the “random layer model" [1]) short-range order (SRO) in PMN [2], but first principles (FP) calculations with sufficiently large supercells to realistically approximate a disordered PMN crystal with SRO are prohibitively time consuming. Relatively small supercells that might reasonably approximate the case of 1:1 SRO include the $[001]_{NCC'}$ structure [3] which was predicted to be the PMN cation-ordering ground state (CGS) [4].

One objective of this study is to fully relax different small PMN supercells consisting of 15 and 30 ions in order to determine their “displacive ground states" (DGS), and to compare their energies, dynamical charges, vibrational frequencies, and infrared (IR) reflectance spectra. These results are important to understand possible effects of local ordering on IR reflectance and Raman spectra.

A second objective to understand the nature of the soft vibrational modes in the ordered structures of PMN. It has been reported that relaxors exhibit both ferroelectric (FE) and antiferroelectric (AFE) characteristics, [5] and that competition between FE and AFE fluctuations is the cause of glass-type properties in PMN.

All FP calculations were done with the Vienna *ab initio* simulation package (VASP) [6]. Several supercells of PMN composition were considered (Fig. 1). Our FP computations show that all these structures are dynamically unstable when the ions are placed on ideal perovskite positions, and full relaxation often leads to surprisingly low symmetry. For example, the FP DGS of the $[001]_{NNM}$ structure (a $[001]_{2:1}$ superlattice) is monoclinic (type M_C [7]), with those Pb close to a Mg plane displaced in the (0.18 Å, 0.05 Å, -0.05 Å) and (0.18 Å, 0.05 Å, 0.05 Å) directions. Those Pb ions which are between the Nb planes are mostly displaced in the x direction by 0.27 Å.

Tetragonal $[001]_{NCC'}$ PMN is also dynamically unstable, and has has a wide spectrum of instabilities that are associated with FE, AFE, octahedral tilting and other modes.

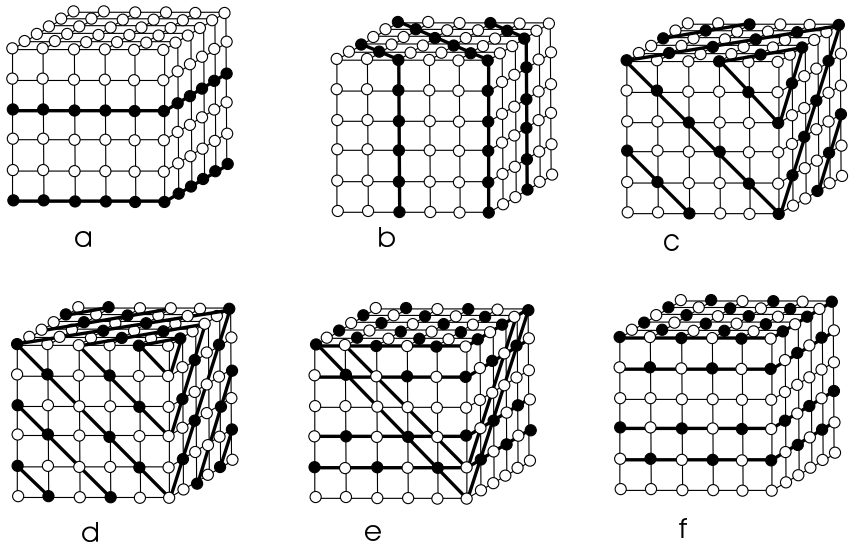

FIGURE 1. PMN structures considered in the present study: $[001]_{NNM}$ (a), $[110]_{NNM}$ (b), $[111]_{NNM}$ (c), $[111]_{NHNH'NH''}$ (d), $[001]_{NCC'NC'C}$ (e), and $[001]_{NCC'}$ (f)

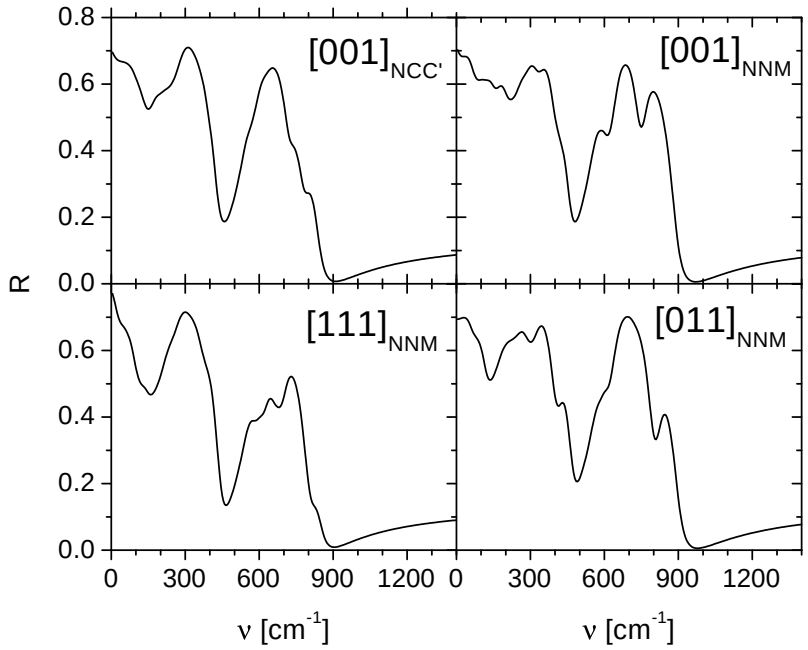

FIGURE 2. Computed IR reflectance spectra for different ordered structures of PMN

TABLE 1. Ionic coordinates (in Å) in the $[001]_{NCC'}$ structure

type	x	y	z	type	x	y	z	type	x	y	z
Mg_1	7.98	-0.02	8.16	Mg_2	4.00	-0.00	4.08	Nb_1	4.01	-0.09	8.11
Nb_2	3.95	-0.04	0.08	Nb_3	7.93	-0.02	0.00	Nb_4	3.99	-3.98	4.12
O_1	2.04	0.40	8.10	O_2	5.96	-0.31	8.04	O_3	4.40	1.98	8.12
O_4	3.66	-1.98	8.10	O_5	2.05	0.17	0.00	O_6	6.03	-0.03	12.02
O_7	4.18	2.01	12.12	O_8	4.00	-1.98	12.07	O_9	1.98	0.00	3.86
O_{10}	6.06	0.06	3.96	O_{11}	4.02	2.06	3.87	O_{12}	4.06	-2.02	3.92
O_{13}	0.27	-0.01	10.21	O_{14}	4.00	-3.92	1.94	O_{15}	0.11	-0.04	6.09
O_{16}	3.97	0.14	10.11	O_{17}	4.12	0.02	1.95	O_{18}	3.95	0.20	6.13
Pb_1	5.75	1.99	10.07	Pb_2	5.96	1.98	2.41	Pb_3	5.84	1.87	6.30
Pb_4	1.89	1.74	10.10	Pb_5	5.95	-2.04	2.40	Pb_6	2.06	1.83	6.27

We relaxed the $[001]_{NCC'}$ structure after a random initial perturbation of the ions. Relaxed coordinates are listed in Table 1. The basis vectors (in Å) are: (4.00, -4.00, 0.00), (4.01, 4.01, 0.01), and (0.00, -0.01, 3×4.07). Relaxations of ionic coordinates are a complex mixture of octahedral deformations around Mg-ions (with rather large frozen angles) plus AFE, and FE, Pb-displacements in opposition to neighboring O-ions. The *x*-direction displacements differ from *y*-direction displacements. Pb-ions have either two, or four, Mg nearest neighbors (nn): Pb-ions with two Mg nn are displaced, by 0.25 Å, towards the centroid of the Mg-Mg nn pair. Pb-ions with four Mg nn are not displaced. We have not proven that the structure in Table 1 is the PMN $[001]_{NCC'}$ DGS (it is possible that relaxation from a different initial perturbation would lead to a state with lower energy). The reported structure is dynamically stable, however, and has lower energy than PMN $[001]_{NCC'}$ that is relaxed with only FE displacements, or only octahedral tilting.

Dynamical charges $Z^\star$ for the $[001]_{NCC'}$ structure are listed in Table 2.[8] For Nb, there is a strong correlation between the number of nn Nb ions and the dynamical charge. Nb ions that have Nb nn in both the $\pm\alpha$ directions have particularly large $Z^\star_{\alpha\alpha}$ (9.11). The two symmetry-independent cases of Nb ions that have one Nb nn in the $\pm\alpha$ directions have $Z^\star_{\alpha\alpha}$ of 6.48 and 7.87, respectively. The Nb ions that have no Nb nn in the $\pm\alpha$ directions have $Z^\star_{\alpha\alpha} = 6.00$. Dynamical charges for Pb also exhibit significant anisotropy, and environment dependence.

TABLE 2. Ionic dynamical charges (in |e|) for PMN $[100]_{NCC'}$ (tetragonal symmetry imposed).

ion i	Z^*_{izz}	Z^*_{ixx}	Z^*_{iyy}	ion i	Z^*_{izz}	Z^*_{ixx}	Z^*_{iyy}	ion	Z^*_{izz}	Z^*_{ixx}	Z^*_{iyy}
Mg_1	2.74	2.65	2.65	Mg_2	2.74	2.65	2.65	Nb_1	6.48	6.00	6.00
Nb_2	7.87	9.11	9.11	Nb_3	7.87	9.11	9.11	Nb_4	6.48	6.00	6.00
O_1	-2.61	-3.62	-2.82	O_2	-2.61	-3.62	-2.82	O_3	-2.61	-2.82	-3.62
O_4	-2.61	-2.82	-3.62	O_5	-1.99	-7.04	-2.09	O_6	-1.99	-7.04	-2.09
O_7	-1.99	-2.09	-7.04	O_8	-1.99	-2.09	-7.04	O_9	-2.61	-3.62	-2.82
O_{10}	-2.61	-3.62	-2.82	O_{11}	-2.61	-2.82	-3.62	O_{12}	-2.61	-3.62	-2.82
O_{13}	-4.15	-2.57	-2.57	O_{14}	-5.71	-2.42	-2.42	O_{15}	-3.93	-2.44	-2.44
O_{16}	-5.71	-2.42	-2.42	O_{17}	-4.15	-2.57	-2.57	O_{18}	-3.93	-2.44	-2.44
Pb_1	3.52	4.41	4.41	Pb_2	3.52	4.41	4.41	Pb_3	4.17	3.93	3.93
Pb_4	3.52	4.41	4.41	Pb_5	3.52	4.41	4.41	Pb_6	4.17	3.93	3.93

TABLE 3. The diagonal frequencies of the dynamical matrix for the 30-ion $[001]_{NCC'}$ supercell of PMN (in cm^{-1}).

ion	z	x	y	ion	z	x	y	ion	z	x	y
Mg_1	346	328	340	Mg_2	276	340	344	Nb_1	279	271	290
Nb_2	322	276	270	Nb_3	318	286	251	Nb_4	301	288	283
O_1	385	537	333	O_2	262	608	251	O_3	399	331	521
O_4	256	267	648	O_5	300	640	248	O_6	263	657	257
O_7	297	272	625	O_8	281	246	633	O_9	292	577	302
O_{10}	281	612	278	O_{11}	285	278	600	O_{12}	279	299	613
O_{13}	555	264	294	O_{14}	661	267	261	O_{15}	735	214	207
O_{16}	557	241	250	O_{17}	733	233	253	O_{18}	596	244	245
Pb_1	108	88	76	Pb_2	81	78	81	Pb_3	93	81	68
Pb_4	105	76	89	Pb_5	88	79	70	Pb_6	92	67	76

For the 30-ion $[001]_{NCC'}$ structure, computed diagonal frequencies of the dynamical matrix are listed in Table 3. The frequencies of Nb-, Mg- and bending O-vibrations are all between 200 cm^{-1} and 350 cm^{-1}. The stretching O-vibrations along Mg-O and Nb-O bonds range from 520 cm^{-1} to 735 cm^{-1}. The Pb diagonal frequencies are in the range from 67 cm^{-1} to 108 cm^{-1}.

As in experiment [9], computed IR reflectance spectra (Fig. 2) consist of three main reststrahlen bands of the vibrational modes that are typical of perovskites: the first group is below 120 cm^{-1}; the second spreads from 150 cm^{-1} to 400 cm^{-1}; and the third is from 500 cm^{-1} to 800 cm^{-1}. The two lower bands split into two subbands each. Assignments of these bands can be made on the basis of the diagonal frequencies shown in Table 3. In experimental data [9], these groups of lines are rather compact as in the computed $[001]_{NCC'}$ and $[111]_{MNN}$ structures. However, the experimentally determined magnitude of the reflectivity in the interval from 500 cm^{-1} to 800 cm^{-1} is lower than in the computation. This could be connected with an overestimation of the oxygen dynamical charge and/or with large damping for some frequencies in this interval (an estimated damping constant of 60 cm^{-1} was used for all frequencies), or it could be that the systems studied here are not sufficiently representative of SRO-disordered PMN.

The lowest calculated optical frequency in the equilibrium 30-ion $[001]_{NCC'}$ structure is 24 cm^{-1}. It is lower than the lowest Pb diagonal frequency (60 cm^{-1}) shown in Table 3 because of the interaction among the ionic vibrations. This mode is basically a perovskite acoustic mode, but has some infrared oscillator strength due to the superlattice Mg-Nb arrangement, which folds certain non-zone center acoustic modes to zone-center IR-active modes. Pb-dominated modes are spread over the interval from 24 cm^{-1} to 129 cm^{-1}. Mostly ferroelectric Pb displacements are at 40 cm^{-1} and 60 cm^{-1} to 90 cm^{-1} although a significant FE contribution to the vibrations exists in the whole interval from 24 cm^{-1} to 129 cm^{-1}. Some modes in this interval are dominated by the displacement of a specific Pb ion (are “quasilocal"). Similarly, some modes in the frequency interval from 500 cm^{-1} to 800 cm^{-1} are dominated by oxygen displacement along a specific Nb-O-Mg bond.

Raman spectra show broad lines with gradual temperature dependence in a wide temperature interval [10, 11]. The presence of these lines would be forbidden if the ions were in symmetric environments. Ionic displacements due to disorder and symmetry

breaking can explain the existence of these Raman lines. A possible measure of the intensities of these lines is the square of the projection of the ionic displacements, from symmetric positions, onto the vibrational modes: $S_i = \left|\langle \mathbf{v}_d | \mathbf{v}_i \rangle\right|^2$, where $\mathbf{v}_d$ is the vector of the frozen displacements, and $\mathbf{v}_i$ is the vector of the *i*-th vibration in the displacements' representation.

Low-frequency Raman lines (about 50 cm^{-1}) are almost certainly due to Pb-O stretching modes [11], and may be associated with the "quasilocal" vibrations described above. Note that, as is typical of Pb-based perovskites that also have large B-cations (*e.g* Mg), Pb-vibrational branches have relatively small dispersion and (for reference structures with Pb ions at ideal perovskite positions) are unstable across most of the Brillouin zone. The particular instabilities that freeze in should depend sensitively on the local electric fields produced by the Nb-Mg configuration. Freezing of lattice instabilities creates low-symmetry Pb-sites, and also allows AFE Pb-vibrations to couple with FE vibrations.

Structural instabilities (which exist in all the supercells studied) also imply that displacive relaxations will reduce their energies relative to the values reported in Burton and Cockayne [4] Column one in Table 4 gives the energies of each structures with symmetry restrictions imposed as in [4] (for example, tetragonal symmetry was imposed for $[001]_{NNM}$ and $[001]_{NCC'}$). Column two gives the relaxed (DGS) energy for each structure. Remarkably, the hierarchy of formation energies and predicted CGS ($[001]_{NCC'}$) remain the same.

There are many possible ordered derivatives of the random layer model [1] that have (111) Nb-layers which alternate with (111) ($Mg_{2/3}Nb_{1/3}$)-layers in which Nb and Mg are ordered; e.g. Fig. 1d. Depending on the projection axis, the mixed layers in this structure are ordered either in stripes, or in an Mg-honeycomb pattern with Nb's at hexagon centers. This structure has a high energy relative to the others in Fig. 1. Perhaps cations in the $Mg_{2/3}Nb_{1/3}$ layers would prefer to have more neighbors of the same species. This is consistent with the conclusion of Hoatson et al.[12] who obtained an improved inverse Monte Carlo fit to NMR data with the assumption of Mg-Mg and Nb-Nb clustering within mixed layers. The structure shown in Fig. 1e also has higher energy than $[001]_{NCC'}$.

TABLE 4. The supercell's energy (in eV per 30-ion supercell)

	ideal structure	relaxed structure
$[001]_{NNM}$	0.825	0.583
$[110]_{NNM}$	0.710	0.155
$[111]_{NNM}$	0.696	0.150
$[001]_{NCC'}$	0.523	0

In summary, our FP computations have shown that the relaxation of the ionic coordinates in the small supercells of PMN does not change the hierarchy of the energy of these structures: $[001]_{NCC'}$ remains the CGS among the small supercells considered. The lowest frequency vibrations in this structure are acoustic modes, but which have nonzero infrared oscillator strengths due to superlattice Mg-Nb ordering. The next-lowest modes are connected with mixed FE-AFE Pb vibrations and with Pb-O stretching modes. The computed IR reflectance spectrum, qualitatively, corresponds to experimental data [9],

although there are some discrepancies in the line magnitudes at high frequencies.

S.A.P. appreciates discussions with J. Toulouse, O. Svitelskiy, J. Petzelt, S. Kamba and Yu. Yuzyuk.

REFERENCES

1. P. K. Davies and M. A. Akbas, J. Phys. Chem. Sol. **61**, 159 (2000).
2. H.B. Krause, J.M. Cowley and J. Wheatley, Acta. Cryst. **A35**, 1015 (1979).
3. All of the structures in this paper are layered structures and can thus be described using the notation $[xyz]_{AB...}$, where *xyz* is the stacking direction and $AB\ldots$ the stacking sequence. In the stacking sequences, *M* refers to a pure Mg layer, *N* to a pure Nb layer, *C* to a $Mg_{1/2}Nb_{1/2}$ "checkerboard" layer, and *H* to a $Mg_{2/3}Nb_{1/3}$ "honeycomb" layer. Where more than one stacking of the same type of layer is possible, primes and double primes distinguish among these stackings.
4. B. P. Burton and E. Cockayne, Ferroelectrics **270**, 173 (2002).
5. T. Egami, Ferroelectrics **267**, 101 (2002).
6. G. Kresse and J. Hafner, Phys. Rev. **B47**, 558 (1993).
7. M_C refers to polarization in the $[ab0]$ direction. See, *e.g.*, figure 2 in L. Bellaiche, A. Garcia, and D. Vanderbilt, Phys. Rev. B **64**, 060103 (2002).
8. To reduce the computational cost associated with the very low symmetry of the DGS, the dynamical charges were calculated with respect to a PMN supercell in which tetragonal symmetry was maintained. The dynamical charges of the atoms will change slightly upon relaxation to the positions in Table 1, and some ions which are symmetry equivalent in Table 2 are not symmetry equivalent in the DGS (Table 1). We assume that the differences between the dynamical charges of the two cases will not significantly affect the calculated IR spectrum in this case.
9. I. M. Reaney, J. Petzelt, V. V. Voitsekhovskii, F. Chu, and N. Setter, J. Appl. Phys. **76**, 2086 (1994).
10. V. I. Torgashev, Yu. I. Yuzyuk, L. T. Latush, P. N. Timonin, and R. Farhi, Ferroelectrics **199**, 197 (1997).
11. E. Husson, L. Abello, and A. Morell, Mat. Res. Bull. **25**, 539 (1990).
12. G.L. Hoatson, D.H. Zhou, F. Fayon, D. Massiot, and R.L. Vold, Phys. Rev. **B66** 224103 (2002).